Journal of Magnetic Resonance 210 (2011) 171–176

Contents lists available at ScienceDirect

Journal of Magnetic Resonance

journal homepage: www.elsevier.com/locate/jmr

Cross relaxation in liquid methanol

J.T. Gerig *

Department of Chemistry & Biochemistry, University of California, Santa Barbara, CA 93106, USA

ARTICLE INFO

Article history:
Received 21 October 2010
Revised 28 February 2011
Available online 6 March 2011

Keywords:
Intermolecular relaxation
MD simulation
Methanol
Cross-relaxation

ABSTRACT

The cross relaxation rate for intermolecular dipole–dipole interactions between methyl protons in liquid methanol at 0 °C was measured and compared to the rate predicted from MD simulations of the experimental system. The experimental and calculated values agree well, even though the translational diffusion coefficient and bulk viscosity of the sample are not well-predicted by the simulations.

1. Introduction

Many attributes of a peptide or protein may be altered by dissolving the biopolymer in a mixture of water and a small organic molecule such as trifluoroethanol or acetonitrile [1–3]. Alterations of solubility, electrophoretic mobility, dominant conformation and propensity for self-assembly can be produced in this way. Direct interactions between the solvent components and the solute are presumably involved to some extent in provoking such changes. Intermolecular NOE experiments have been used to explore details of interactions between organic cosolvents and dissolved peptides [4–6].

Theories for the intermolecular NOE are typically based on hard sphere models and bulk properties of solution components. In many cases, estimates of intermolecular cross-relaxation rates made using these approaches are close to experimental results. For peptides dissolved in organic-water mixtures, disagreements between observed and calculated cross relaxation rates can be taken as indicating (1) selective accumulation of a solvent component near a spin of interest or (2) alteration of the local dynamics of solvent–solute interactions. However, hard sphere models rarely support interpretations of experimental results that are unique or offer details at the molecular level. Molecular dynamics simulations have developed to the point that reasonably reliable predictions of properties of organic solvents and water-organic mixtures are practical [7–10]. MD methods may, thus, offer a better way of understanding solvent spin–solute spin interactions reflected in intermolecular NOE experiments.

Cross relaxation in neat methanol has been studied as a prelude to application of MD methods to interpretation of intermolecular NOE results obtained previously in this laboratory [5,6,11,12]. A mixture of carbon-13 labeled methanol and normal methanol was used to determine the intermolecular cross relaxation rate ($\sigma_{CH_3CH_3}$) arising from interactions between methyl protons of the liquid. A sample temperature of 0 °C was used since most of the peptide systems of interest were examined at this temperature. The experimental results are compared to predictions derived from MD simulations of the experimental system.

2. Results

2.1. Experimental determination of $\sigma_{CH_3CH_3}$

Fig. 1 shows the methyl region of the proton spectrum of a mixture of CH_3OH and $^{13}CH_3OH$, with CD_3OH present to provide a lock signal. The center $^{12}CH_3OH$ signal was selectively inverted and changes in intensity of the adjacent signals of the $^{13}CH_3OH$ species were detected as a function of mixing time. A typical plot of intermolecular NOE vs. mixing time is shown in Fig. 2. The initial slope of the plot defines $\sigma_{CH_3CH_3}$ for interaction of $^{12}CH_3$ methyl protons with the $^{13}CH_3$ group [13].The value of $\sigma_{CH_3CH_3}$ found was $5.2 \pm 0.2 \times 10^{-3}\ s^{-1}$, with the uncertainty estimated by considering the reproducibility of multiple experiments.

2.2. Diffusion

The translational diffusion coefficients (D_{trans}) at 0 °C of both methanol species shown in Fig. 1 were found to be $1.47 \pm 0.07 \times 10^{-9}\ m^2\ s^{-1}$, in agreement with the results of O'Reilly and Peterson [14] and Price et al. [15].

* Fax: +1 805 893 2113.
E-mail address: gerig@chem.ucsb.edu

1090-7807/$ - see front matter © 2011 Elsevier Inc. All rights reserved.
doi:10.1016/j.jmr.2011.03.002

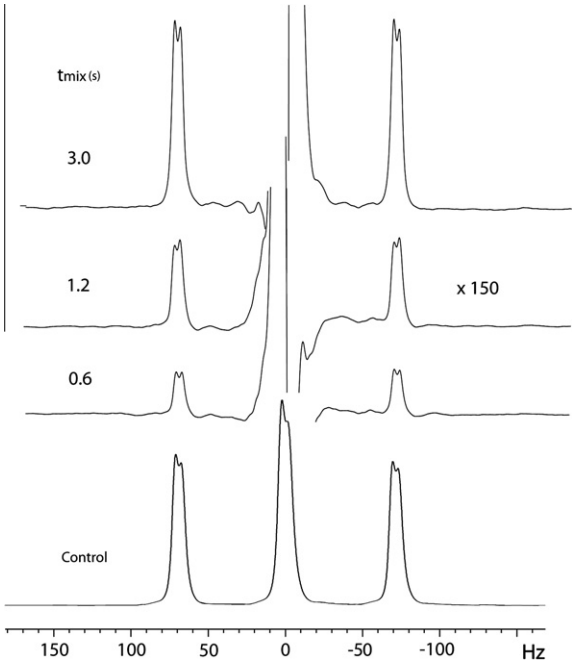

Fig. 1. Proton NMR spectra at 0 °C of the mixture of methanol isotopomers described in the experimental section. The unperturbed spectrum of the methyl region is shown at the bottom; intermolecular NOE spectra at the mixing times indicated, produced by inverting the central $^{12}CH_3OH$ signal, appear above. The vertical scale factor for each NOE spectrum is 150 times larger than that of the control. Enough of the center signal remains in the NOE spectra that there is some baseline distortion at the carbon-13 satellites. This was reduced by subtracting a spectrum obtained at a short mixing time. The apparent $^3J_{CHOH}$ coupling constant at this temperature is 4.4 Hz.

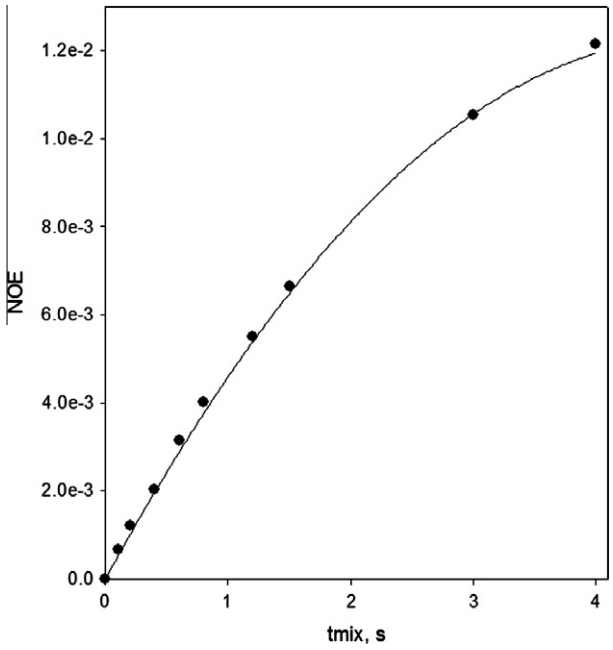

Fig. 2. A typical plot of the intermolecular NOE produced on the methyl carbon-13 lines in the CD_3OH–CH_3OH–$^{13}CH_3OH$ mixture described in the text when the methyl resonance of CH_3OH is inverted. The initial slope of the curve, which can be equated to $\sigma_{CH_3CH_3}$, was estimated by fitting the function $y = a * t_{mix} + b * t_{mix}^2$ to the data, with the initial slope taken as the value of the parameter *a*.

2.3. Properties of methanol at 0 °C from MD simulations

Wensink et al. reported MD studies of methanol at 25 °C that led to computed densities and heats of vaporization in agreement with experimental results, although transport properties were less well predicted. The force field and general approach of these authors were adopted for the present work. It was confirmed that the heat of vaporization, system density, translational diffusion coefficient and molecular reorientation time (τ_2) of liquid methanol computed from simulations done in our laboratory replicated the values of these quantities at 25 °C published by Wensink et al.

Table 1 presents bulk properties at 0 °C calculated from MD simulations done with various samples of methanol. Results from at least three independent simulations were averaged to give the entries in the Table. The computed density of pure methanol at 0 °C is about 1% less than the experimental value, similar to the discrepancy between observed and predicted density at 25 °C [9].

Many studies have found that the translational diffusion coefficient (D_{trans}) obtained from simulations of ~200 methanol molecules agree with the corresponding experimental result [19–22]. In our work, the translational diffusion coefficient at 0 °C increased somewhat as the number of methanol molecules in a simulation increases from 200 to 16,000. Dependence of D_{trans} at 25 °C on the number of molecules present has been reported [23]. We find that computed diffusion coefficients for simulations of 2000 or more methanol molecules exceed the experimental value by 15–20% at both 0 and 25 °C. Isotopomers of methanol had the same calculated diffusion coefficients in mixtures of these species.

In contrast, the viscosity (η) computed from simulations was 40–50% less than the experimental value. Computed viscosities were, again, found to be sensitive to the number of molecules in a simulation at 0 and 25 °C, increasing significantly as the number of molecules increased (Table 1).

The re-orientational autocorrelation function $P_2\langle\vec{e}(t)\cdot\vec{e}(0)\rangle$ of a unit vector directed along the C–O axis of a methanol molecule was calculated. Integration of the normalized autocorrelation function yields the re-orientational correlation time τ_2. Based on the second-order Legendre polynomial, τ_2 potentially would be used in characterizing NMR relaxation experiments. Our simulations at 25 °C gave a value for τ_2 in agreement with that reported by Wensink et al. [9]; an increase of τ_2 at 0 °C is expected. While relaxation in a variety of isotopic forms of methanol have been reported in NMR studies [24,25], the roles of aggregation and hydrogen bonding makes attribution of experimental observations to specific modes of methanol re-orientation challenging. It appears that no unambiguous experimental NMR determination of τ_2 at 0 °C is available for comparison to the predicted value in Table 1. Interpolation of the quasielastic neutron scattering data of Bermejo et al., gives $\tau_2 \approx 1.4 \pm 0.9$ ps at 0 °C [26].

2.4. Calculation of intermolecular cross relaxation rates

Abragam has shown that the spin–lattice relaxation rate R_1 and cross relaxation rate σ_{AB} arising from the dipolar interaction of a pair of distinguishable spin ½ particles A and B are given by Eqs. (1) and (2) [27].

$$R_1 = \frac{1}{T_1} = \frac{3}{4}\gamma_A^2\gamma_B^2\hbar^2\left\{\frac{1}{12}j^0(\omega_A-\omega_B)+\frac{3}{2}j^1(\omega_A)+\frac{3}{4}j^2(\omega_A+\omega_B)\right\} \quad (1)$$

$$\sigma_{AB} = \frac{3}{4}\gamma_A^2\gamma_B^2\hbar^2\left\{-\frac{1}{12}j^0(\omega_A-\omega_B)+\frac{3}{4}j^2(\omega_A+\omega_B)\right\} \quad (2)$$

Table 1
Properties of methanol at 0 °C from simulations.

Number of CH_3OH molecules	200	2000	2000 mix[a]	16,000 mix[b]	Experimental values
Box side (nm)[c]	2.363	5.095	5.094	10.190	
Density (gl^{-1})	806.8 ± 0.4	804.7 ± 0.1	827.1 ± 0.2	826.5 ± 0.1	810.2 [16] 810.4 [17] 825. (mix)[d]
D_{trans}, $\times 10^9$ m^2 s^{-1}	1.57 ± 0.10	1.72 ± 0.07	1.79 ± 0.11[e] 1.75 ± 0.05 1.70 ± 0.02	1.84 ± 0.07[e] 1.83 ± 0.02 1.83 ± 0.06	1.59 [15] 1.51 [14] 1.41 [18]
η, $\times 10^3$ P	3.71 ± 0.05	5.21 ± 0.15	5.37 ± 0.02	6.26 ± 0.34	8.08 [16] 7.97 [17]
τ_2 (ps)	2.8 ± 0.1	2.6 ± 0.1	2.7 ± 0.1	2.7 ± 0.1	

[a] System consisted of 250 CD_3OH, 750 CH_3OH and 1000 $^{13}CH_3OH$ molecules.
[b] System consisted of 2000 CD_3OH, 6000 CH_3OH and 8000 $^{13}CH_3OH$ molecules.
[c] Length of an edge of the cubic simulation box.
[d] Density calculations for mixtures assumed that the density of all isotopomers have the same temperature dependence as CH_3OH and that there is no volume change upon mixing.
[e] Values given are for CD_3OH, CH_3OH and $^{13}CH_3OH$ species, respectively.

Here, γ is the proton gyromagnetic ratio and ω_A and ω_B are the corresponding Larmor frequencies. The spectral density functions $j^m(\omega)$ are Fourier transforms of correlation functions $g^m(t)$ which can be written in terms of the components of the vector **r** which connects the two spins [28]

$$j^m(\omega) = 2\int_0^\infty g^m(t)e^{-i\omega t}dt = 2\int_0^\infty \left\langle F^m(0)F^{m^*}(t)\right\rangle e^{-i\omega t}dt \tag{3}$$

with

$$F^0 = \frac{r^2-3z^2}{r^5} \quad F^1 = \frac{z(x-iy)}{r^5} \quad F^2 = \frac{(x-iy)^2}{r^5}$$

Random isotropic motion of the vector **r** is assumed, with the average of the quantity $F^m(0)F^{m^*}(t)$ appearing in Eq. (3).

Provided that cross correlation effects can be neglected [29,30], the collective relaxation contributions of a group of identical B spins interacting with a target A spin is given by

$$R_1 = \frac{3}{4}\gamma_A^2\gamma_B^2\hbar^2\left\{\frac{1}{12}J^0(\omega_A-\omega_B)+\frac{3}{2}J^1(\omega_A)+\frac{3}{4}J^2(\omega_A+\omega_B)\right\} \tag{4}$$

and

$$\sigma_{AB} = \frac{3}{4}\gamma_A^2\gamma_B^2\hbar^2\left\{-\frac{1}{12}J^0(\omega_A-\omega_B)+\frac{3}{4}J^2(\omega_A+\omega_B)\right\}$$

with

$$J^m(\omega) = 2\int_0^\infty G^m(t)e^{-i\omega t}dt = 2\int_0^\infty \left\{\frac{1}{N_{target}}\sum_i^{N_{target}}\sum_{j\neq i}^{N_{cut}}F_{ij}^m(0)F_{ij}^m(t)\right\}e^{-i\omega t}dt \tag{5}$$

The right summation in Eq. (5) collects all pair-wise interactions with a particular target spin. The number of spins involved in these interactions (N_{cut}) may be limited by imposition of a cut-off radius. The collected interactions are averaged over all target spins (N_{target}). The strong internuclear distance dependence of $G^m(t)$ dictates that R_1 and σ_{AB} are dominated by interactions of a given target spin with its near-neighbors. The correlation functions $G^m(t)$ are expected to be real functions [27] and this expectation has been confirmed in computational studies [31].

For isotropic liquids, normalized correlation functions ($G^m(t)/G^m(0)$) are independent of m and normalized $G^0(t)$, $G^1(t)$and $G^2(t)$ show the same time dependence [27]. Following Feller et al. [32], we have assumed that the normalized functions can be represented by a collection of n exponentially decaying functions. By approximating the decay of $G^m(t)/G^m(0)$ by a sum of exponentials, the Fourier transform of $G^m(t)$ becomes

$$J^m(\omega) = 2G^m(0)\tau_m(\omega) \tag{6}$$

with

$$\tau_m(\omega) = \sum_n \frac{a_n\tau_n}{\left(1+(\omega\tau_n)^2\right)} \tag{7}$$

where $\sum a_n = 1$. The largest values of τ_n observed in any of the analyses done for the present work were of the order 330 ps and, at the experimental operating frequency (500 MHz), the extreme narrowing approximation does not apply.

2.5. Calculation of $\sigma_{CH_3CH_3}$ for methanol from simulations

Intermolecular dipolar relaxation in liquid methanol depends on all pair-wise interactions in the sample. Ideally, when predicting relaxation from a MD simulation, the summations shown in Eq. (5) would extend over a very large number of spins. However, there are practical limits to how many molecules can be included in a simulation. Moreover, the calculation of pair-wise interactions according to Eq. (5) becomes highly time-consuming as the number of molecules increases.

At some point, the distance between a pair of protons is so large that their interaction contributes little to the sum in Eq. (5). Computation of $G^m(t)$ can thus be accelerated by imposing a cut-off radius to limit the number of spins considered to be involved with a given target spin. We imagine a sphere of radius r_{cut} centered on a particular methanol CH_3 proton. The subsequent motions of protons that are present within the selection

Table 2
Calculated cross relaxation rate for CD_3OH–CH_3OH–$^{13}CH_3OH$ mixtures at 0 °C.[a]

Total molecules	Number of $^{13}CH_3OH$ target spins[b]	$G^0(0)/G^1(0)$	$G^2(0)/G^1(0)$	$\sigma_{CH_3CH_3}$, $\times 10^3$ s^{-1}
2000	3000	5.97 ± 0.04	3.98 ± 0.03	5.6 ± 0.2
16,000	612[c]	6.01 ± 0.04	4.00 ± 0.08	5.6 ± 0.1
16,000	24,000	5.98 ± 0.01	4.00 ± 0.02	5.5 ± 0.1

[a] The quantities given are averages of results obtained from 4 or more trajectory segments of 500–600 ps duration obtained from the last half of 3 or more independent simulations of 2 ns length. Standard deviations are appended. A cut-off distance of 3.0 nm was used for all calculations. There are 1925 CH_3OH methyl protons in a sphere of this radius.
[b] The number of $^{13}CH_3OH$ methyl protons in the simulation box that are target spins for the dipole–dipole calculation.
[c] Spins within the central 3 nm × 3 nm × 3 nm volume of the simulation box were selected as target spins.

sphere at time = 0 relative to the target proton are assumed to produce the intermolecular relaxation of the target spin. Given a large enough cut-off radius, the number and behavior of spins selected by this procedure should be sufficient to reproduce the relaxation behavior of a macroscopic sample. It was determined for the mixture of methanol isotopomers that values of r_{cut} larger than 2.5 nm gave essentially the same computed relaxation rates for liquid methanol.

Table 2 gives the results of calculations of $\sigma_{CH_3CH_3}$ done using trajectories produced by MD simulations of the mixture of CD_3OH, CH_3OH and $^{13}CH_3OH$ molecules described earlier. All calculations reported used r_{cut} = 3.0 nm. With simulations of 2000 methanol molecules, a 3.0 nm cut-off produces a sphere of interacting CH_3OH around some $^{13}CH_3OH$ target spins that includes spins in replica cells defined by the periodic boundary conditions. It is possible that coordination of the motions of molecules in the central simulation box with those of molecules in replicas could influence the calculated correlation functions [31]. To check for such influences, calculations were done using trajectories obtained from simulations of 16,000 molecules. Target $^{13}CH_3OH$ molecules were taken only from a 3 nm × 3 nm × 3 nm cube in the center of the simulation box. In this case, all CH_3OH molecules selected by r_{cut} = 3.0 nm are well within the central simulation box and periodic influences from the replicas should be absent or highly reduced. There was essentially no difference between $\sigma_{CH_3CH_3}$ calculated by these approaches, or when all of the target $^{13}CH_3OH$ molecules in the central simulation box of 16,000 molecule simulations were considered (Table 2). The average of all calculations indicated $\sigma_{CH_3CH_3}$, estimated from simulations, is $5.6 \pm 0.1 \times 10^{-3}$ s^{-1}.

It is expected that $G^2(0) = 4 \cdot G^1(0)$ and $G^0(0) = 6 \cdot G^1(0)$for an isotropic system [27]. The ratios $G^2(0)/G^1(0)$ and $G^0(0)/G^1(0)$ were monitored throughout our calculations. As shown in Table 2, the observed ratios were close to the expected values.

3. Discussion

MD simulations following the procedures of Wensink et al. [9] afford good predictions of the heat of vaporization and density of methanol at 25 °C. However, simulations were less successful in predicting dynamic properties such as translational diffusion and bulk viscosity at 25 °C, as has previously noted by these authors. After confirming the results at 25 °C reported by Wensink et al., use of their protocol led to a predicted density for methanol at 0 °C that was within about 1% of the experimental value. Again, diffusion and viscosity at this temperature were not accurately predicted (Table 1).

There is an inverse relation between the translational diffusion coefficient of a liquid and viscosity [21,23,33–35]. Thus, underestimates of the viscosity of methanol at 0 and 25 °C by the MD simulations are qualitatively consistent with overestimated of translational diffusion coefficients. However, predictions of both parameters depend on the number of molecules simulated and there appears to be no simple relationship between the calculated diffusion coefficients and sample viscosity.

The force field used for the simulations reported here does not include the effects of electronic polarization. It has been found in other systems that failure to include polarizability can lead to underestimation of diffusion and over-prediction of viscosity [36–39]. There are reports that a more elaborate force field that takes into account molecular polarizability improves the predicted diffusion coefficient and viscosity of methanol [22,34,35]. but most of those studies involved simulations of only 200–500 molecules of methanol. Given the dependence of D_{trans} and η on the number of molecules reported here (Table 1), it would be of interest to explore the effects of molecular polarizability in larger simulations.

A hard sphere model of liquid methanol can be used to estimate the intermolecular cross relaxation parameter $\sigma_{CH_3CH_3}$ in the mixture studied. Assuming rapid molecular reorientation, each proton of a methanol molecule is considered to be located at the center of a sphere of radius r_M [40]. The results of Ayant et al. [41] show that $\sigma_{CH_3CH_3}$ arising from interactions of the CH_3OH methyl protons with methyl protons of $^{13}CH_3OH$ is given by

$$\sigma_{CH_3CH_3} = \frac{3\gamma_H^4 h^2 N_S}{10\pi D r}\left(6J_2(2\omega_H) - J_2(0)\right) \tag{8}$$

where ω_H is the proton Larmor frequency, N_S is the number of inverted CH_3OH spins per mL, D is the sum of the diffusion coefficients, assumed to be equal for the CH_3OH and $^{13}CH_3OH$ molecules ($D = 2D_{CH_3OH}$), r is the distance of closest approach of the spheres representing these species ($r = 2r_M$) and $J_2(\omega)$ is a spectral density function given in equation (9),

$$J_2(\omega) = \left(\frac{\omega\tau + \frac{5}{\sqrt{2}}(\omega\tau)^{1/2} + 4}{(\omega\tau)^3 + 4\sqrt{2}(\omega\tau)^{5/2} + 16(\omega\tau)^2 + 27\sqrt{2}(\omega\tau)^{3/2} + 81\omega\tau + 81\sqrt{2}(\omega\tau)^{1/2} + 81}\right) \tag{9}$$

with the correlation time $\tau = \frac{r^2}{D}$. Assuming that the radius of a methanol molecule is 0.208 nm [6] and that D_{CH_3OH} is the experimental value reported above, Eq. (8) gives 4.6×10^{-3} s^{-1} for the methyl–methyl cross relaxation rate at 0 °C, in reasonable accord with the experimental result and predictions from MD simulations. Using the larger diffusion coefficient predicted by the MD simulations gives 3.9×10^{-3} s^{-1}. Other results of Ayant et al. can be used to calculate $\sigma_{CH_3CH_3}$ using a model in which the protons of methanol are, on average, displaced some distance from the rotational center of the molecule. It was shown that such models can lead to an increase in the predicted cross relaxation rate. For example, assuming that the average location of the methyl protons is 0.1 nm from the center and that the rotational diffusion constant of the molecule is $\frac{1}{6\tau_2}$ [33], leads to $\sigma_{CH_3CH_3} = 5.0 \times 10^{-3}$ s^{-1}.

4. Conclusions

MD simulations done using a conventional force field lead to a predicted intermolecular cross relaxation rate for dipole–dipole interactions of the methyl protons in liquid methanol that is close to the experimental value at 0 °C. This outcome is somewhat surprising since the simulations do not produce particularly good predictions of the translational diffusion coefficient or bulk viscosity. However, we note that Luhmer et al. have reported that MD simulations of xenon-129 dissolved in benzene produced a cross relaxation rate due to interactions of solvent protons with Xe that agreed with experiment [28]. Error compensation effects may be at play here and it would be of interest to understand them better. For the present, it appears reasonable, given a sufficiently reliable force field, to expect intermolecular cross relaxation parameters

for solvent–solute interactions estimated through MD simulations to agree reasonably well with experiment.

5. Experimental

5.1. Materials

CH_3OH (anhydrous, 99.8%), $^{13}CH_3OH$ (99 atom %) and CD_3OH (99.9 atom %) were used as received from Sigma–Aldrich. A mixture of these components with the molar ratios 2.9:3.9:1.0, respectively, was prepared and sealed in a J. Young tube (Wilmad) under atmospheric pressure.

5.2. Instrumentation and experimental procedures

Proton NMR spectra were collected at 500 MHz using a Varian INOVA instrument and a Nalorac triple resonance probe equipped with xyz pulsed field gradient coils. Pulse sequences used for the intermolecular NOE experiments were based on those published by Dalvit [42], except that an excitation sculpting scheme [43,44] with 15 Hz bandwidth square pulses was used for selective inversion of the CH_3OH signal at the start of the NOE mixing time, rather than the approach described by Dalvit. A computational study of the selectivity of this inversion based on the Bloch equations suggested that the intensities of the signals from $^{13}CH_3OH$ were altered less than 1% by inversion of the CH_3OH line. Mixing times for intermolecular NOE experiments ranged from 50 to 4000 ms. Sample temperatures were determined using the observed shift difference between OH and $^{12}CH_3$ methyl signals of the sample and a standard calibration curve [45]. (http://www.spectroscopynow.com/FCKeditor/UserFiles/File/specNOW/HTML%20files/NMR_temperature_measurement.htm). Temperatures are believed to have been constant to better than ±0.1 °C during the course of an experiment and accurate to better than ±0.5 °C.

Plots of the intermolecular NOE vs. mixing time were analyzed as described previously [13,46]. The derived cross relaxation parameter ($\sigma_{CH_3CH_3}$) for interaction of $^{12}CH_3OH$ and $^{13}CH_3OH$ methyl protons was corrected for the extent of inversion of the $^{12}CH_3OH$ signal.

Self-diffusion coefficients of sample components were determined by bipolar double stimulated echo pulsed field gradient experiments [47], following procedures previously described [5]. Pulsed field gradients were calibrated using doped 1% H_2O in D_2O sample (Varian) and the data of Longsworth [48].

5.3. MD simulations

All simulations were done with the GROMACS package [49,50] running on a SUN SunFire X4600. The force field and overall approach of Wensink et al. was used [9]. Systems examined included 200 and 2000 molecules of CH_3OH and a total of 2000 or 16,000 molecules of a mixture of CD_3OH, CH_3OH and $^{13}CH_3OH$, with the isotopic species present in the ratio 1:3:4, respectively. Force field parameters for isotopically enriched species were assumed to be the same as those for CH_3OH. A cubic simulation cell was used, with periodic boundary conditions applied. Motion of the model center of mass was corrected every 0.01 ps. Snapshots of the system coordinates and velocities typically were written every 50 or 100 fs. Covalent bonds were kept at constant length by the SHAKE procedure since it was observed that removing these constraints had virtually no effect on the calculated cross relaxation parameters. The integration time-step was 0.002 ps. Cut-offs for electrostatic and van der Waals terms were 1.1 nm [9]. The PME method for long-range electrostatics was applied, as was the long-range correction for the van der Waals interaction described by Allen and Tildesley [51].

Simulations were regulated at 298 or 273 °C and a pressure of 1 bar by use of the Berendsen temperature (velocity re-scaling) and pressure coupling methods with relaxation time constants of 0.1 and 1 ps, respectively [52].

After initial equilibration for at least 500 ps, simulations of trajectories of 2 ns duration were carried out, with analyses of system properties done using the last half of the trajectory created. Programs contained within the GROMACS package were used to compute the system density, self-diffusion coefficients from the mean square molecular displacement using the Einstein relationship [53], viscosity through calculation of transverse current autocorrelations [54], and molecular re-orientation times.

Fitting of $\frac{G^m(t)}{G^m(0)}$ computed from a MD trajectory to a sum of exponential functions used a local version of Provencher's program DISCRETE [55]. (See http://s-provencher.com/index.shtml.) The program systematically tried sums of up to eight terms, with the best fit selected according to criteria discussed by Provencher. Typically, the best fit consisted of 5 or 6 exponential terms.

Acknowledgments

We thank the National Science Foundation of support of the initial phases of this work (Grant CHE-0408415) and the authors and developers of GROMACS for making their software available.

References

[1] W. Sirikun, N. Vardhanabhuti, N. Sutanthavibul, Organic solvent and acid induced conformational modification of model peptide: lysozyme, Solid State Phenom. 121–123 (2007) 759–762.
[2] N. Chaudhary, S. Singh, R. Nagaraj, Organic solvent mediated self-association of an amyloid forming peptide from beta 2-microglobulin: an atomic force microscopy study, Biopolymers 90 (2008) 783–791.
[3] M. Buck, Trifluoroethanol and colleagues: cosolvents come of age. Recent studies with peptide and proteins, Q. Rev. Biophys. 31 (1998) 297–355.
[4] M. Fioroni, M.D. Diaz, K. Burger, S. Berger, Solvation phenomena of a tetrapeptide in water/trifluoroethanol and water/ethanol mixtures: a diffusion NMR, intermolecular NOE and molecular dynamics study, J. Am. Chem. Soc. 124 (2002) 7737–7744.
[5] C. Chatterjee, D. Martinez, J.T. Gerig, Interactions of trifluoroethanol with [val^5] angiotensin II, J. Phys. Chem. B 111 (2007) 9355–9362.
[6] R.C. Neuman Jr., J.T. Gerig, Interaction of alcohols with [Val^5] angiotensin in alcohol–water mixtures, J. Phys. Chem. B 114 (2010) 6722–6731.
[7] W.L. Jorgensen, D.S. Maxwell, J. Tirado-Rives, Development and testing of the OPLS all-atom force field on conformational energetics and properties of organic liquids, J. Am. Chem. Soc. 118 (1996) 11225–11236.
[8] R.D. Mountain, K.A. Lippa, Solvation of perfluorooctane and octane in water, methanol, acetonitrile, and aqueous mixtures of methanol and acetonitrile, J. Phys. Chem. B 112 (2008) 7785–7793.
[9] E.J.W. Wensink, A.C. Hoffmann, P.J. van Maaren, D. van der Spoel, Dynamic properties of water/alcohol mixtures studied by computer simulation, J. Chem. Phys. 119 (2003) 7308–7317.
[10] C. Oldiges, K. Wittler, T. Tonsing, A. Alijah, MD calculated structural properties of clusters in liquid acetonitrile/water mixtures with various contents of acetonitrile, J. Phys. Chem. A 106 (2002) 7147–7154.
[11] D.P. Chagolla, J.T. Gerig, Conformations of betanova in aqueous trifluoroethanol, Biopolymers 93 (2010) 893–903.
[12] J.T. Gerig, Structure and solvation of melittin in 1,1,1,3,3,3-hexafluoro-2-propanol/water, Biophys. J. 86 (2006) 3166–3175.
[13] J.T. Gerig, Solute-solvent interactions probed by intermolecular NOEs, J. Org. Chem. 68 (2003) 5244–5428.
[14] D.E. O'Reilly, E.M. Peterson, Self-diffusion coefficients and rotational correlation times in polar liquids. II, J. Chem. Phys. 55 (1971) 2155–2163.
[15] W.S. Price, H. Ide, Y. Arata, Solutions dynamics in aqueous monohydric alcohol systems, J. Phys. Chem. A 107 (2003) 4784–4789.
[16] R.C. Weast, CRC Handbook of Chemistry and Physics, 44th Ed (1962).
[17] F. Kurata, T.W. Yergovich, G.W. Swift, Density and viscosity of aqueous solutions of methanol and acetone from the freezing point to 10 °C, J. Chem. Eng. Data 16 (1971) 222–226.
[18] R.E. Rathbun, A.L. Babb, Self diffusion in liquids. III. Temperature dependence in pure liquids, J. Phys. Chem. 65 (1961) 1072–1074.
[19] E. Hawlicka, G. Palinkas, K. Heinzinger, A molecular dynamics study of liquid methanol with a flexible six-site model, Chem. Phys. Lett. 1989 (1989) 255–259.

[20] G. Palinkas, I. Bako, K. Heinzinger, P. Bopp, Molecular dynamics investigation of the inter- and intramolecular motions in liquid methanol and methanol–water mixtures, Mol. Phys. 73 (1991) 897–915.
[21] E. Guardia, G. Sese, J.A. Padro, Of the hydroden bonding effects in liquid methanol: A molecular dynamics simulation study, J. Mol. Liq. 62 (1994) 1–16.
[22] S. Patel, C.L. Brooks III, A nonadditive methanol force field: Bulk liquid and liquid–vapor interfacial properties via molecular dynamics simulations using a fluctuating charge model, J. Chem. Phys. 122 (2005) 024508-024501–024508-024509.
[23] I.M.J.J. van de Ven-Lucassen, T.J.H. Vlugt, A.J.J. van der Zanden, P.J.A.M. Kerkhof, Molecular dynamics simulation of self-diffusion and Maxwell-Stefan diffusion coefficients in liquid mixtures of methanol and water, Mol. Simul. 223 (1999) 79–94.
[24] H. Versmold, NMR studies of the reorientational motion in methanol and methanol–water mixtures, Ber. Bunsenges Phys. Chem. 84 (1980) 168–173.
[25] H.G. Hertz, The problem of intramolecular rotation in liquids and nuclear magnetic relaxation, Prog. NMR Spectrosc. 16 (1983) 115–162.
[26] F.J. Bermejo, F. Batallan, E. Enciso, R. White, A.J. Dianoux, W.S. Howells, Diffusional dynamics in hydrogen-bonded liquids: methanol, J. Phys. Condens. Matter 2 (1990) 1301–1314.
[27] A. Abragam, The Principles of Nuclear Magnetism, Oxford, Oxford, 1961.
[28] M. Luhmer, A. Moschos, J. Reisse, Intermolecular dipole-dipole spin relaxation of xenon-129 dissolved in benzene. A molecular dynamics simulation study, J. Magn. Reson. A 113 (1995) 164–168.
[29] G. Lippens, D. Van Belle, S.J. Wodak, J. Jeener, T_1 relaxation time of water from a molecular dynamics simulation of water, Mol. Phys. 80 (1993) 1469–1484.
[30] M. Odelius, A. Laaksonen, M.H. Levitt, J. Kowalewski, Intermolecular dipole–dipole relaxation. A molecular dynamics simulation, J. Magn. Reson. A 105 (1993) 289–294.
[31] J.-P. Grivet, NMR relaxation parameters of a Lennard-Jones fluid from molecular dynamics simulations, J. Chem. Phys. 123 (2005) 034503.
[32] S.E. Feller, D. Huster, K. Gawrisch, Interpretation of NOESY cross-relaxation rates from molecular dynamics simulation of a lipid bilayer, J. Am. Chem. Soc. 121 (1999) 8963–8964.
[33] J.H. Noggle, R.E. Schirmer, The Nuclear Overhauser Effect, Academic, New York, 1971.
[34] L.X. Dang, T.-M. Chang, Many-body interactions in liquid methanol and its liquid/vapor interface. A molecular dynamics study, J. Chem. Phys. 119 (2003) 9851–9857.
[35] Y. Zhong, G.L. Warren, S. Patel, Thermodynamic and structural properties of methanol–water solutions using nonadditive interaction models, J. Comput. Chem. 29 (2007) 1142–1152.
[36] T. Yan, C.J. Burnham, M.G. Del Popolo, G.A. Voth, Molecular dynamics simulation of ionic liquids. The effect of electronic polarizability, J. Phys. Chem. B 108 (2004) 11877–11881.
[37] C. Rey-Castro, L.F. Vega, Transport properties of the ionic liquid 1-ethyl-3-methylimidazolium chloride from equilibrium molecular dynamics simulations. The effect of temperature, J. Phys. Chem. B 110 (2006) 14426–14435.
[38] D.P. Geerke, W.F. van Gunsteren, The performance of non-polarizable and polarizable parameter sets for ethylene glycol in molecular dynamics simulations of the pure liquid and its aqueous mixtures, Mol. Phys. 105 (2007) 1861–1881.
[39] O. Borodin, Polarizable force field development and molecular dynamics simulations of ionic liquids, J. Phys. Chem. B 2009 (2009) 11463–11478.
[40] G. Otting, E. Liepinsh, B. Halle, U. Frey, NMR indentification of hydrophobic cavities with low water occupancies in protein structures using small gas molecules, Nat. Struct. Biol. 4 (1997) 396–404.
[41] Y. Ayant, E. Belorizky, P. Fries, J. Rosset, Effet des interactions dipolaires magnetiques intermoleculaires sur la relaxation nucleaire de molecules polyatomiques dans les liquides, J. Phys. Fr. 38 (1977) 325–337.
[42] C. Dalvit, Efficient multiple-solvent suppression for the study of the interactions of organic solvents with biomolecules, J. Biol. NMR 11 (1998) 437–444.
[43] T.L. Hwang, A.J. Shaka, Water suppression that works. Excitation sculpting using arbitrary wave-forms and pulsed-field gradients, J. Magn. Reson. A 112 (1995) 275–279.
[44] K. Stott, J. Stonehouse, J. Keeler, T.L. Hwang, A.J. Shaka, Excitation sculpting in high-resolution nuclear magnetic resonance spectroscopy: application to selective NOE experiments, J. Am. Chem. Soc. 117 (1995) 4199–4200.
[45] C. Amman, P. Meier, A.E. Merbach, A simple multinuclear NMR thermometer, J. Magn. Reson. 46 (1982) 319–321.
[46] J.T. Gerig, NOE studies of solvent–solute interactions, Annu. Rep. NMR Spectrosc. 64 (2008) 21–75.
[47] A. Jerschow, N.J. Muller, Suppression of convection artifacts in stimulated-echo diffusion experiments. Double stimulated-echo experiments, J. Magn. Reson. 125 (1997) 372–375.
[48] L.G. Longsworth, The mutual diffusion of light and heavy water, J. Phys. Chem. 64 (1960) 1914–1917.
[49] D. van der Spoel, E. Lindahl, B. Hess, G. Groenhof, A.E. Mark, H.J.C. Berendsen, GROMACS: Fast, flexible and free, J. Comput. Chem. 26 (2005) 1701–1718.
[50] B. Hess, C. Kutzner, D. van der Spoel, E. Lindahl, GROMACS 4: algorithms for highly efficient, load-balanced and scalable molecular simulation, J. Chem. Theory Comput. 4 (2008) 435–447.
[51] M.P. Allen, D.J. Tildesley, Computer Simulations of Liquids, Oxford, Oxford, 1987.
[52] X. Grabuleda, C. Jaime, P.A. Kollman, Molecular dynamics simulation studies of liquid acetonitrile: new six-site model, J. Comput. Chem. 21 (2000) 901–908.
[53] A.R. Leach, Molecular Modeling – Principles and Applications, 2nd ed., Pearson Prentice Hall, Harlow, England, 2001.
[54] B.J. Palmer, Transverse-current autocorrelation-function calculations of the shear viscosity for molecular liquids, Phys. Rev. E 49 (1994) 359–366.
[55] S.W. Provencher, An eigenfunction expansion method for the analysis of exponential decay curves, J. Chem. Phys. 64 (1976) 2772–2777.